https://doi.org/10.5194/egusphere-2026-6152
Preprint. Discussion started: 12 November 2026
© Author(s) 2026. CC BY 4.0 License.

# A process-based representation of hydraulic activation of stomata induced by hygroscopic fertilizer salts in the ORCHIDEE-CROP model (v2.2)

**Authors**

Shuaishuai Deng [1], Jürgen Burkhardt [2], Ronny Lauerwald [1], Christophe Flechard [3], Jürgen Knauer [4], Benjamin Dumont [5], Emilio Baud-Fraile [1], Yang Su [1], Ke Yu [6], Nicolas Viovy [7], Benjamin Loubet [1]

**Affiliations**

[1] UMR ECOSYS, INRAE AgroParisTech, Université Paris-Saclay, 91120 Palaiseau, France
[2] Institute of Crop Science and Resource Conservation, University of Bonn, Bonn, Germany
[3] UMR 1069 SAS, INRAE, Institut Agro, Rennes, 35042, France
[4] School of Life Sciences, Faculty of Science, University of Technology Sydney, Ultimo, NSW 2007, Australia
[5] ULiege-Gembloux AgroBio-Tech, Plant Sciences Axis, Crop Science Lab., B-5030 Gembloux, Belgium
[6] International Institute for Applied Systems Analysis (IIASA), Schlossplatz 1, 2361 Laxenburg, Austria
[7] Laboratoire des Sciences du Climat et de l'Environnement, IPSL, CEA-CNRS-UVSQ, Université Paris-Saclay, Gif-sur-Yvette, France

**Corresponding author**

Shuaishuai Deng shuaishuai.deng@inrae.fr +33 7 66 57 34 52 Université Paris-Saclay

https://doi.org/10.5194/egusphere-2026-6152
Preprint. Discussion started: 12 November 2026
© Author(s) 2026. CC BY 4.0 License.

**Abstract**

Hydraulic activation of stomata (HAS) induced by hygroscopic salt films on leaf surfaces can create an additional liquid water loss pathway beyond conventional stomatal vapor diffusion. However, this process is not represented in current land surface and crop models. Using the practice-relevant example of hygroscopic urea ammonium nitrate (UAN) application to field crops, we developed a process-based parameterization of UAN-induced HAS in the ORCHIDEE-CROP model. The scheme represents event-based UAN retention, prognostic HAS storage, dry depletion, rainfall wash-off, and a relative humidity-dependent effective wet fraction, which is incorporated into the latent heat flux (LE) partitioning framework through an additional evaporative efficiency term. The parameterization was calibrated using event-scale transpiration anomalies from a winter wheat site and evaluated at three winter wheat sites and one maize site using eddy covariance (EC) observations and crop management records. The scheme produced transient post-UAN HAS responses, with declining HAS storage and event-specific wetting dynamics. Including HAS increased simulated mean LE during the 0–10 d post-UAN period by 2.0–4.0% across the four study sites, while soil water feedback reduced plant transpiration, partially offsetting the direct HAS water loss, with mean offset fractions ranging from 13.3% to 24.9% across sites. Comparison with EC observations showed that including HAS tended to reduce negative LE bias when the standard model underestimated observed LE. Simulated gross primary productivity remained nearly unchanged, whereas increased LE reduced simulated inherent water-use efficiency by 4.0–5.3% across the four study sites. These results demonstrate the feasibility of representing UAN-induced HAS as an event-driven, meteorologically regulated process and provide a basis for extending the framework to hygroscopic aerosol effects in land surface and crop models.

**Keywords:** hydraulic activation of stomata; hygroscopic fertilizer salts; crop water use; ORCHIDEE-CROP; land surface model; latent heat flux; eddy covariance

## 1 Introduction

Plant transpiration is commonly represented in land surface and crop models as a stomatally regulated process, in which water vapor diffuses from the substomatal cavity to the atmosphere (Farquhar et al., 1980; Ball et al., 1987; Medlyn et al., 2011). This framework underlies the simulation of carbon–water exchange across scales (Krinner et al., 2005; Beer et al., 2009; Bonan, 2019). However, it implicitly assumes that leaf water loss is controlled by stomatal aperture and occurs primarily through vapor diffusion. This assumption may neglect an additional water loss pathway involving liquid water transfer associated with hygroscopic leaf surface material (HLSM; Burkhardt, 2010; Burkhardt et al., 2012; Grantz et al., 2018).

The hydraulic activation of stomata (HAS) hypothesis proposes that HLSM, including deposited atmospheric aerosols and agricultural sprays, can form thin aqueous films through deliquescence; these films may penetrate stomatal pores and connect with internal apoplastic water, thereby extending the plant hydraulic system to the leaf surface (Burkhardt et al., 1995; Burkhardt and Pariyar, 2014; Burkhardt et al., 2018). Under such conditions, part of the internal plant water may be transported through thin liquid films and evaporate from the leaf surface (Burkhardt, 2010; Grantz et al., 2018). This pathway differs from conventional canopy

https://doi.org/10.5194/egusphere-2026-6152
Preprint. Discussion started: 12 November 2026
© Author(s) 2026. CC BY 4.0 License.

interception evaporation because it involves water loss that may remain hydraulically connected to the leaf interior. Experimental evidence has shown that hygroscopic salts and aerosols can promote leaf surface wetness and increase transpiration, consistent with HAS-related responses (Burkhardt and Pariyar, 2016; Burkhardt et al., 2023; Frank et al., 2025). More broadly, recent evidence shows that fine particulate pollution can reduce plant water-use efficiency primarily by suppressing photosynthesis rather than altering evapotranspiration, underscoring the broader ecological relevance of aerosol effects on plant carbon–water exchange (Wang et al., 2026). In agricultural systems, hygroscopic urea ammonium nitrate (UAN) fertilizers are widely used (Lu and Tian, 2017; Cao et al., 2018). During spray application, a fraction of UAN can be intercepted by the crop canopy, providing a practice-relevant source of HLSM. UAN can remain liquid even at 20% relative humidity (RH) (Weston et al., 2003), potentially facilitating the formation and persistence of hygroscopic films on treated leaf surfaces (Tredenick et al., 2022; Barlas et al., 2023). Consistent with this mechanism, Deng et al. (2026) provided field evidence for UAN-induced HAS in winter wheat and maize, where UAN application was associated with increased vegetation conductance and generally stronger responses in transpiration than in gross primary productivity (GPP). The magnitude and duration of UAN-induced HAS are likely controlled by UAN retention and persistence, RH-dependent wetting, and rainfall wash-off, suggesting that the process should be represented as event-driven and meteorologically regulated. Despite its potential relevance to managed agricultural systems, HAS remains largely overlooked in land surface and crop models.

ORCHIDEE-CROP simulates crop phenology, carbon assimilation, transpiration, soil evaporation, and canopy interception processes (Wu et al., 2016; Müller et al., 2017; Wang et al., 2017; Yin et al., 2020; Fu et al., 2023). However, it does not explicitly represent hygroscopic UAN residues on canopy surfaces. This limitation constrains the simulation of short-term deviations in crop water fluxes following UAN application, which are not captured by standard transpiration and interception schemes. Such additional water loss may be particularly relevant during drought and other water-limited conditions, when short-term increases in crop water use could affect soil water availability and subsequent plant water use. In this study, we implement a process-based parameterization of UAN-induced HAS in ORCHIDEE-CROP. The new scheme represents event-based UAN retention, a prognostic HAS storage variable, dry depletion, rainfall wash-off, and an RH-dependent effective wet fraction. This wet fraction is incorporated into the existing latent heat flux (LE) partitioning framework as an additional evaporative efficiency term. The parameterization is applied at three winter wheat sites and one maize site with UAN applications, using EC observations and crop management records.

The objectives of this study are therefore to (1) develop a canopy-scale representation of UAN-induced HAS in ORCHIDEE-CROP; (2) calibrate the parameterization against event-scale transpiration anomalies and evaluate its performance using EC observations; and (3) assess the influence of key empirical parameters and soil water limitation on simulated HAS-related water loss. By incorporating this previously neglected HAS-related water loss pathway into a process-based model, this study provides a first step toward representing UAN-induced HAS in land surface modeling and evaluating its implications for crop carbon–water exchange

https://doi.org/10.5194/egusphere-2026-6152
Preprint. Discussion started: 12 November 2026
© Author(s) 2026. CC BY 4.0 License.

under managed agricultural conditions.

## 2 Data and methods

The methodological framework comprises meteorological forcing and crop management data (Sect. 2.1), a description of the ORCHIDEE-CROP model (Sect. 2.2), the newly implemented HAS parameterization (Sect. 2.3), parameter calibration and sensitivity analysis (Sect. 2.4), model simulations (Sect. 2.5), and model evaluation (Sect. 2.6). An overview of the workflow is provided in Fig. 1.

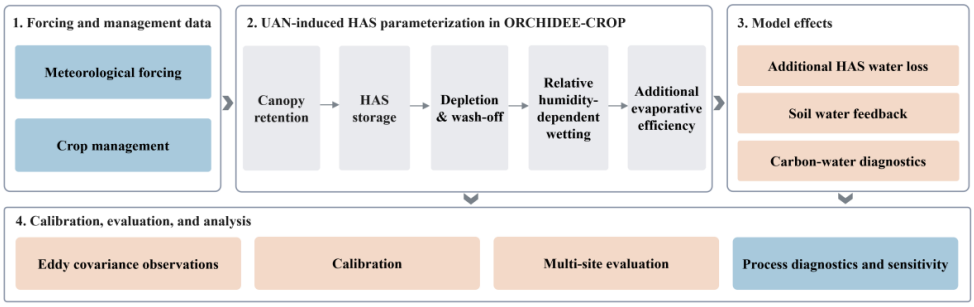



**Figure 1.** Overview of the implementation, calibration, and evaluation of urea ammonium nitrate (UAN)-induced hydraulic activation of stomata (HAS) in ORCHIDEE-CROP. Meteorological forcing and crop management data drive the event-based HAS parameterization, which represents canopy retention, HAS storage, depletion and wash-off, relative humidity-dependent wetting, and additional evaporative efficiency. The resulting additional HAS water loss is coupled to the soil water balance, allowing feedback on conventional transpiration. The framework includes calibration against eddy covariance observations, multi-site evaluation of ORC-HAS against ORC-STD, and process diagnostics and sensitivity analyses.

### 2.1 Forcing and crop management data

Meteorological forcing data for ORCHIDEE-CROP were derived from eddy covariance (EC) observations at four temperate cropland sites with urea ammonium nitrate (UAN) liquid fertilizer application records. The dataset comprised half-hourly winter wheat observations from three ICOS sites (FR-Gri, BE-Lon, and FR-EM2) and hourly maize observations from one AmeriFlux site (US-Ne1) (Table S1). The meteorological variables included incoming shortwave and longwave radiation (W $m^{-2}$), surface pressure (Pa), rainfall rate (kg $m^{-2}$ $s^{-1}$), snowfall rate (kg $m^{-2}$ $s^{-1}$), near-surface air temperature (K), near-surface specific humidity (kg $kg^{-1}$), and near-surface wind speed (m $s^{-1}$). Available crop management information, including sowing and harvest dates and UAN application dates and rates, is summarized by site in Tables S2–S5.

### 2.2 Overview of the ORCHIDEE-CROP model

ORCHIDEE-CROP is a branch of the process-based land surface model ORCHIDEE (Krinner et al., 2005) that incorporates modules from the STICS crop model, including crop phenology, crop management, and a simplified nitrogen fertilization scheme (Brisson et al., 2003, 2009; Wu et al., 2016). ORCHIDEE-CROP has

https://doi.org/10.5194/egusphere-2026-6152
Preprint. Discussion started: 12 November 2026
© Author(s) 2026. CC BY 4.0 License.

subsequently been applied and evaluated in regional and global assessments of crop phenology, climate impacts, and water management (Müller et al., 2017, 2019; Wang et al., 2017, 2021; Yin et al., 2020; Fu et al., 2023). It simulates biophysical and biogeochemical processes in croplands, including carbon and water fluxes, crop growth, and yield. In this study, we used a version calibrated against leaf area index (LAI), flowering and harvest dates, crop yield, and crop residues for winter wheat and maize (Su et al., 2025; Yu et al., 2026).

#### 2.2.1 Crop growth and development

Crop development in ORCHIDEE-CROP follows the STICS phenology scheme described by Wu et al. (2016). For winter wheat and maize, the crop module simulates crop development using stage-specific growing degree day (GDD) requirements derived from STICS, while the timing and duration of each stage are further modified by photoperiod, vernalization, and environmental limitations such as water stress. Phenological transitions occur when the corresponding GDD thresholds are reached. Maturity and harvest are determined based on accumulated GDD and grain water content. The harvest criterion was calibrated for wheat and maize using crop phenology observations from the Deutscher Wetterdienst (DWD) in Germany (Su et al., 2025).

#### 2.2.2 Surface energy budget

As in most land surface models, the surface energy budget in ORCHIDEE-CROP is expressed as:

$$R_n = \mathrm{LE} + H + G \quad (1)$$

where $R_n$ is net radiation (W m$^{-2}$), LE is latent heat flux (W m$^{-2}$), $H$ is sensible heat flux (W m$^{-2}$), and $G$ is ground heat flux (W m$^{-2}$). The partitioning of LE follows a $\beta$-based framework (Wu et al., 2016; Yu et al., 2026). Under non-snow and non-flooded conditions relevant to the present cropland simulations, LE is calculated as:

$$\mathrm{LE} = \lambda \rho_a C_d u \beta [q_{sat}(T_s) - q_a] \quad (2)$$

where $\lambda$ is the latent heat of vaporization (J kg$^{-1}$), $\rho_a$ is air density (kg m$^{-3}$), $C_d$ is the dimensionless aerodynamic exchange coefficient, $u$ is wind speed (m s$^{-1}$), $q_{sat}(T_s)$ is the saturation specific humidity (kg kg$^{-1}$) at surface temperature ($T_s$), $q_a$ is near-surface air specific humidity (kg kg$^{-1}$), and $\beta$ is the dimensionless evaporative efficiency. In the standard model, $\beta$ combines the contributions from canopy interception loss, transpiration, and bare soil evaporation:

$$\beta = \beta_2 + \beta_3 + \beta_4 \quad (3)$$

where $\beta_2$, $\beta_3$, and $\beta_4$ are dimensionless evaporative efficiency terms representing canopy interception loss, transpiration, and bare soil evaporation, respectively. Snow sublimation is treated separately through $\beta_1$. The implementation of the original $\beta$ terms is summarized in Table S6.

https://doi.org/10.5194/egusphere-2026-6152
Preprint. Discussion started: 12 November 2026
© Author(s) 2026. CC BY 4.0 License.

## 2.3 New parameterization for HAS in ORCHIDEE-CROP

### 2.3.1 Event-based UAN canopy retention

To represent UAN-induced HAS on canopy surfaces, we introduced an event-based HAS storage scheme into ORCHIDEE-CROP. UAN was applied over the managed crop area according to the site-specific application dates and rates. ORCHIDEE-CROP uses a fixed annual fertilizer amount of 100 kg N $ha^{-1}$ to calculate a static fertilizer limitation factor and does not explicitly simulate nitrogen dynamics. UAN applications were used only to drive canopy HAS storage and did not alter this background fertilizer setting. For each UAN application event, the initially retained UAN amount, $N_{ret}$ (kg N $m^{-2}$), was calculated using the prescribed throughfall fraction:

$$N_{\mathrm{ret}} = (1 - f_{\mathrm{tf}})N_i \quad (4)$$

where $f_{tf}$ is the throughfall fraction of applied UAN, assumed constant at 0.7 based on EFSA (2017), and $N_i$ is the applied UAN amount for event $i$ (kg N $m^{-2}$). $N_{ret}$ was then converted into a dimensionless increment, $\Delta S_{HAS}$, to update the normalized canopy HAS storage state $S_{HAS}$ (0–1):

$$\Delta S_{\mathrm{HAS}} = 1 - \exp\left(-\frac{N_{\mathrm{ret}}}{N_{\mathrm{ref}}}\right) \quad (5)$$

where $N_{ref}$ is a reference UAN amount (kg N $m^{-2}$) that controls the conversion from canopy UAN retention to normalized HAS storage and was calibrated as described in Sect. 2.4.1. When $N_{ret} = N_{ref}$, $\Delta S_{HAS} = 1 - e^{-1} \approx 0.63$. At each UAN application event, the prognostic HAS storage was updated as:

$$S_{\mathrm{HAS}}(t) = \min[1, S_{\mathrm{HAS}}(t - \Delta t) + \Delta S_{\mathrm{HAS}}] \quad (6)$$

where $S_{HAS}$ was initialized at 0, $S_{HAS}$ $(t)$ denotes the HAS storage at the current time step, and $\Delta t$ is the time-step duration (d).

### 2.3.2 Depletion and wash-off of HAS storage

Following UAN application, $S_{HAS}$ decreases through first-order dry depletion and rainfall wash-off. The prognostic HAS storage was updated as:

$$S_{\mathrm{HAS}}(t) = S_{\mathrm{HAS}}(t - \Delta t)(1 - f_{\mathrm{wash}})\exp(-\frac{\Delta t}{\tau}) \quad (7)$$

where the dry-depletion timescale $\tau$ (d) represents canopy HAS storage persistence under rain-free conditions and was set to 5 d for the reference simulation (Table 1). $f_{wash}$ is the fraction of $S_{HAS}$ removed by rainfall wash-off. The wash-off fraction was parameterized as a function of canopy interception overflow:

$$f_{\mathrm{wash}} = 1 - \exp(-k_{\mathrm{wash}} q_{\mathrm{overflow}}) \quad (8)$$

where $q_{overflow}$ is the canopy interception overflow during the time step (kg $m^{-2}$), and $k_{wash}$ is the wash-off coefficient ($m^2$ $kg^{-1}$) controlling wash-off sensitivity to canopy interception overflow, with a reference value of 0.30 $m^2$ $kg^{-1}$ (Table 1). When no canopy overflow occurs, $f_{wash} = 0$, and $S_{HAS}$ decreases only through dry depletion.

### 2.3.3 Effective wet fraction and evaporative contribution of HAS

The effective HAS wet fraction, $f_{wet,HAS}$, representing the modeled canopy wetting available for HAS-related

https://doi.org/10.5194/egusphere-2026-6152
Preprint. Discussion started: 12 November 2026
© Author(s) 2026. CC BY 4.0 License.

evaporation, was controlled by relative humidity (RH) and $S_{HAS}$. The RH response followed the empirical relationship reported by Burkhardt et al. (2009), which relates normalized leaf wetness to RH based on leaf wetness observations and Brunauer–Emmett–Teller (BET) theory (Brunauer et al., 1938):

$$LW = 3.68 \times 10^{-4} \exp(7.9RH) \quad (9)$$

where LW is the dimensionless normalized leaf wetness signal and RH is expressed as a dimensionless fraction (0–1). Since LW represents leaf-level wetness rather than a directly observed canopy wet fraction, it was scaled by an empirical RH scaling coefficient, $c_{RH}$, and modulated by $S_{HAS}$ to calculate $f_{wet,HAS}$:

$$f_{wet,HAS} = \min(1 - f_{int},\ c_{RH} S_{HAS} LW) \quad (10)$$

where $c_{RH}$ is dimensionless and was set to 10 for the reference simulation (Table 1), and $f_{int}$ is the fraction of canopy area occupied by intercepted rainfall. The term $(1 - f_{int})$ prevents double counting with intercepted rainfall already represented in the canopy water storage scheme.

To represent UAN-induced HAS within the LE partitioning framework, $\beta_{HAS}$ was added to Eq. (3) and calculated as:

$$\beta_{HAS} = f_{wet,HAS} f_{crop} f_{res} \quad (11)$$

where $f_{crop}$ is the LAI-dependent crop cover fraction within the grid cell, and $f_{res}$ is the dimensionless canopy exchange limitation factor. $\beta_{HAS} = 0$ when either $f_{wet,HAS} = 0$ or $f_{crop} = 0$. $f_{res}$ follows the resistance-based formulation already implemented in ORCHIDEE-CROP (Krinner et al., 2005; Wu et al., 2016):

$$f_{res} = \frac{1}{1 + c_d u (r_{veget} + r_{struct})} \quad (12)$$

where $r_{veget}$ and $r_{struct}$ are the vegetation and structural resistances (s m$^{-1}$), respectively. The HAS flux was included in the soil water balance, so that HAS-induced changes in soil moisture could indirectly affect soil water stress, conventional transpiration, and gross primary productivity (GPP) through the existing model formulations. The reference HAS parameter values and sensitivity settings are summarized in Table 1.

**Table 1.** Reference HAS parameter values and sensitivity settings.

| Parameter | Description | Unit | Reference value | Sensitivity values | Basis |
|---|---|---|---|---|---|
| $f_{tf}$ | Throughfall fraction of applied UAN | - | 0.7 | Not varied | Prescribed fraction used to derive canopy UAN retention (EFSA, 2017) |
| $N_{ref}$ | Reference retained UAN amount controlling conversion to normalized HAS storage | kg N m$^{-2}$ | 0.001 | Not varied | Calibrated at FR-Gri; fitted retained UAN amount = 0.00091 kg N m$^{-2}$, rounded to 0.001 kg N m$^{-2}$ |

https://doi.org/10.5194/egusphere-2026-6152
Preprint. Discussion started: 12 November 2026
© Author(s) 2026. CC BY 4.0 License.

| Parameter | Description | Unit | Reference value | Sensitivity values | Basis |
|---|---|---|---|---|---|
| $c_{RH}$ | Scaling coefficient for RH-dependent canopy HAS wet fraction | - | 10 | 5, 10, 15 | Empirical canopy-scale scaling; reference value gives near-saturation at RH ≈ 0.7 |
| $\tau$ | Characteristic dry depletion timescale of canopy HAS storage | d | 5 | 3, 5, 7 | Based on the 2.88 d e-folding timescale used in previous ammonia exchange parameterizations, increased to represent longer persistence of UAN-derived hygroscopic material |
| $k_{wash}$ | Wash-off coefficient for HAS storage removal by canopy interception overflow | $m^2$ $kg^{-1}$ | 0.3 | 0.1, 0.3, 1.0 | Weak, reference, and strong wash-off scenarios |

## 2.4 Parameter calibration and sensitivity analysis

### 2.4.1 Calibration of the reference UAN amount

$N_{ref}$ controls the conversion from retained UAN to normalized HAS storage (Eq. 5), but cannot be directly constrained because canopy UAN retention was not measured. We therefore calibrated an applied-UAN equivalent, $N_{ref,app}$, against EC-derived event-scale additional water loss and subsequently converted it to $N_{ref}$ using the prescribed retention fraction. Event-scale additional water loss was estimated from EC-derived ($T_{EC}$) and simulated ($T_{sim}$) transpiration rates (kg $m^{-2}$ $s^{-1}$). $T_{EC}$ was inferred using the LE partitioning approach described in Deng et al. (2026) and subjected to the same data-quality and rainfall filtering, while $T_{sim}$ was obtained from the standard ORCHIDEE-CROP model without the HAS parameterization. For each UAN event, 10 d pre- and post-event windows were used for baseline estimation and anomaly accumulation, respectively. A linear relationship between hourly $T_{EC}$ and $T_{sim}$ was fitted using the pre-event data:

$$T_{EC}(t) = k_1 T_{sim}(t) + k_2, t \in \text{pre} \quad (13)$$

where $k_1$ and $k_2$ are event-specific regression coefficients, with $k_1$ dimensionless and $k_2$ expressed in kg $m^{-2}$ $s^{-1}$. The fitted relationship was then applied to $T_{sim}$ during the 10 d post-event period to estimate the baseline transpiration, $T_{base}$ (kg $m^{-2}$ $s^{-1}$):

$$T_{base}(t) = k_1 T_{sim}(t) + k_2, t \in \text{post} \quad (14)$$

The relationship was fitted separately for each event to account for differences in phenology, meteorological forcing, and structural model bias. Post-event transpiration anomalies, $\Delta T_{HAS}$ (kg $m^{-2}$ $s^{-1}$), were calculated

https://doi.org/10.5194/egusphere-2026-6152
Preprint. Discussion started: 12 November 2026
© Author(s) 2026. CC BY 4.0 License.

as:

$$\Delta T_{\mathrm{HAS}}(t) = T_{\mathrm{EC}}(t) - T_{\mathrm{base}}(t), t \in \mathrm{post} \quad (15)$$

Event-scale additional water loss potentially attributable to HAS, $W_{\mathrm{HAS},i}$, was estimated by accumulating only positive anomalies:

$$W_{\mathrm{HAS},i} = \sum_{t\in\mathrm{post}} \max\left(\Delta T_{\mathrm{HAS}}(t), 0\right)\Delta t \quad (16)$$

where $W_{\mathrm{HAS},i}$ is given in kg m$^{-2}$ for event $i$. The resulting $W_{\mathrm{HAS},i}$ estimates were fitted against the applied UAN amount $N_i$ using a bounded saturating dose–response function:

$$W_{\mathrm{HAS},i} = W_{\mathrm{max}}\left(1 - e^{(-N_i/N_{\mathrm{ref,app}})}\right) \quad (17)$$

where $W_{\mathrm{max}}$ represents the effective upper bound of event-scale additional water loss (kg m$^{-2}$), and $N_{\mathrm{ref,app}}$ is the reference applied UAN amount controlling the saturation of the dose–response function. The parameters were fitted to wheat UAN events at FR-Gri using bounded nonlinear least squares, with $N_{\mathrm{ref,app}}$ constrained between 0.0001 and 0.015 kg N m$^{-2}$ (1–150 kg N ha$^{-1}$). The fitted $N_{\mathrm{ref,app}}$ was 0.00303 kg N m$^{-2}$. Parameter uncertainty was assessed using 1000 bootstrap replicates and an Akaike information criterion (AIC) profile across the constrained range of $N_{\mathrm{ref,app}}$ (Fig. S1). Pooling winter wheat UAN events across FR-Gri, BE-Lon, and FR-EM2 as a cross-site robustness check yielded an $N_{\mathrm{ref,app}}$ of 0.00209 kg N m$^{-2}$. The FR-Gri estimate was used for the reference parameterization. Because Eq. (5) is formulated in terms of retained rather than applied UAN, the $N_{\mathrm{ref,app}}$ fitted at FR-Gri was converted to $N_{\mathrm{ref}}$ using the retained fraction $1 - f_{\mathrm{tf}}$ ($f_{\mathrm{tf}}$ = 0.7; EFSA, 2017). This yielded $N_{\mathrm{ref}}$ = 0.00091 kg N m$^{-2}$, which was rounded to 0.001 kg N m$^{-2}$ for the reference simulations. This value was applied to BE-Lon and FR-EM2 to test transferability across wheat sites, and to US-Ne1 maize as an exploratory application because the available maize UAN events did not support robust crop-specific calibration.

#### 2.4.2 Sensitivity analysis of $c_{\mathrm{RH}}$, $\tau$, and $k_{\mathrm{wash}}$

Sensitivity analyses were conducted for the three empirical HAS parameters $c_{\mathrm{RH}}$, $\tau$, and $k_{\mathrm{wash}}$. The reference value $c_{\mathrm{RH}}$ = 10 was selected empirically to allow $f_{\mathrm{wet,HAS}}$ to approach its upper bound at approximately RH = 0.7 when $S_{\mathrm{HAS}}$ = 1 and $f_{\mathrm{int}}$ = 0. Sensitivity simulations used $c_{\mathrm{RH}}$ = 5, 10, and 15 to assess the sensitivity of RH-dependent wetting.

The reference value $\tau$ = 5 d was based on the 2.88 d e-folding time (i.e., the time required for a first-order reservoir to decline to approximately 37% of its initial value) used in previous ammonia exchange parameterizations (Massad et al., 2010; Flechard et al., 2013), with an expert-based increase to account for the expected longer persistence of UAN-derived hygroscopic material on canopy surfaces. Sensitivity simulations used $\tau$ = 3, 5, and 7 d.

The reference value $k_{\mathrm{wash}}$ = 0.3 m$^2$ kg$^{-1}$ was selected as an intermediate wash-off setting due to the lack of direct observational constraints. Sensitivity simulations used $k_{\mathrm{wash}}$ = 0.1, 0.3, and 1.0 m$^2$ kg$^{-1}$ to represent weak, reference, and strong wash-off removal, respectively.

https://doi.org/10.5194/egusphere-2026-6152
Preprint. Discussion started: 12 November 2026
© Author(s) 2026. CC BY 4.0 License.

### 2.5 Model simulations

Model simulations were conducted for the selected winter wheat and maize growing seasons with UAN applications (Tables S2–S5). For each site–crop combination, ORCHIDEE-CROP was forced by site-specific meteorological observations and prescribed crop management records. We compared two model configurations: the standard ORCHIDEE-CROP simulation without HAS (ORC-STD) and the simulation including the HAS parameterization (ORC-HAS). UAN application dates and rates were used to drive the HAS parameterization in ORC-HAS. ORC-HAS used the reference parameter values and sensitivity settings for $c_{RH}$, $\tau$, and $k_{wash}$ summarized in Table 1. To assess whether water limitation modulated the simulated HAS effect, an additional water-deficit sensitivity experiment was conducted by prescribing the dimensionless soil moisture stress factor *humrel* = 0.5 in both ORC-STD and ORC-HAS.

### 2.6 Model evaluation

The main evaluation window covered 0–10 d after each UAN application and was truncated when necessary to avoid overlap with subsequent applications. Window-length sensitivity was assessed using 0–7 d and 0–14 d windows for the comparison of LE performance between ORC-STD and ORC-HAS, while parameter sensitivity simulations were evaluated using the 0–10 d window. All model outputs and EC observations used for event-scale evaluation were aggregated from the original forcing time step to a daily time step. Event-composite LE dynamics were compared among EC observations, ORC-STD, and ORC-HAS. Event-scale LE performance was quantified using root mean square error (RMSE), mean absolute error (MAE), absolute bias, and $R^2$, and changes in model performance were calculated as ORC-HAS minus ORC-STD.

The internal HAS response was diagnosed using simulated $S_{HAS}$, $f_{wet,HAS}$, and $\beta_{HAS}$. To diagnose the effect of coupling HAS water loss to the soil water balance, the transpiration response was decomposed into direct HAS water loss, the net transpiration difference between ORC-HAS and ORC-STD, and the indirect soil water feedback defined as the net difference minus the direct HAS flux. For each UAN event, the fraction of direct HAS water loss offset by soil water feedback was quantified over the 0–10 d post-UAN period as the cumulative soil water feedback relative to the cumulative direct HAS water loss. Additional diagnostics included simulated $H$, $T_s$, surface relative humidity ($RH_s$; dimensionless), surface vapor pressure deficit ($VPD_s$; kPa), and *humrel* to characterize the surface energy, microclimatic, and soil water responses. Inherent water-use efficiency (IWUE; g C kPa $kg^{-1}$ $H_2O$) was calculated as GPP × VPD / ET, where GPP is expressed in g C $m^{-2}$ $d^{-1}$ and ET denotes evapotranspiration (kg $H_2O$ $m^{-2}$ $d^{-1}$). Observed IWUE was calculated using VPD from the EC dataset, whereas simulated IWUE was calculated using simulated $VPD_s$. IWUE was used as a diagnostic of carbon gain relative to water loss under atmospheric demand (Beer et al., 2009). Detailed diagnostics were presented for FR-Gri and BE-Lon, the two winter wheat sites with the largest numbers of UAN events, while all four sites were included in the multi-site evaluation of post-UAN LE responses and associated changes in IWUE.

https://doi.org/10.5194/egusphere-2026-6152
Preprint. Discussion started: 12 November 2026
© Author(s) 2026. CC BY 4.0 License.

## 3 Results

### 3.1 Simulated HAS dynamics and soil water feedback

The simulated HAS variables showed transient responses following UAN application at both FR-Gri and BE-Lon (Fig. 2a–c). Median $S_{HAS}$ peaked around day 1 and subsequently declined throughout the 0–10 d post-UAN event window. $f_{wet,HAS}$ generally decreased over the event window, with higher values at BE-Lon. $\beta_{HAS}$ followed a temporal pattern similar to that of $f_{wet,HAS}$, with greater contributions during the early post-application period.

Including HAS water loss in the soil water balance produced a consistent transpiration response at both sites (Fig. 2d–e). Direct HAS water loss remained positive throughout the post-UAN period, while reduced *humrel* (Fig. S2) constrained conventional transpiration, resulting in negative soil water feedback that partially offset direct HAS water loss (Fig. 2d–f). These changes were accompanied by increased LE and $RH_s$, together with decreased $H$, $T_s$, and $VPD_s$ in ORC-HAS relative to ORC-STD (Fig. S2).

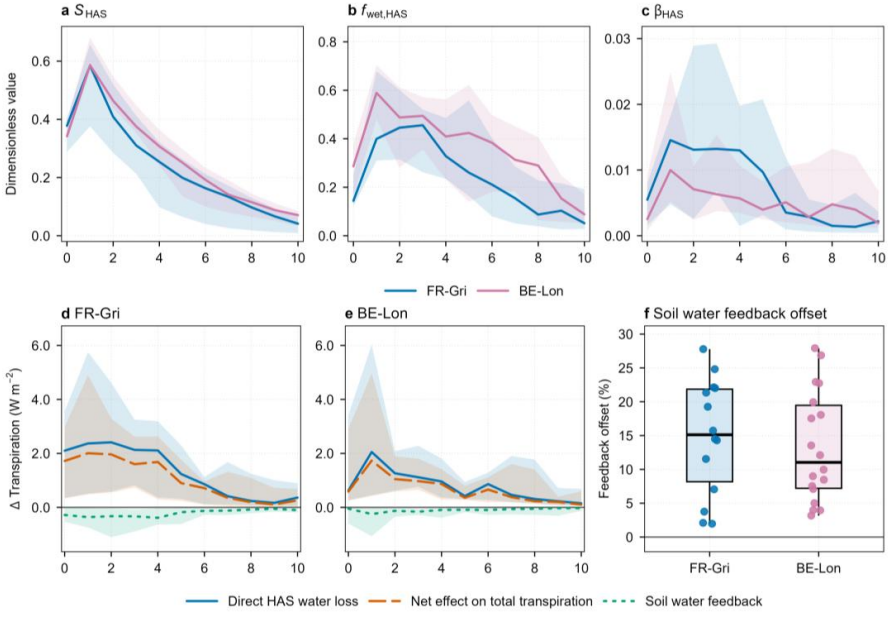



**Figure 2.** Simulated HAS dynamics and transpiration responses following UAN application at FR-Gri and BE-Lon. Panels (a–c) show event-composite responses of $S_{HAS}$, $f_{wet,HAS}$, and $\beta_{HAS}$ over the 0–10 d post-UAN period. Panels (d–e) show the decomposition of the transpiration response at FR-Gri and BE-Lon, respectively. Lines indicate event medians and shaded ribbons indicate interquartile ranges across UAN events. Panel (f) shows the event-scale fraction of direct HAS water loss offset by soil water feedback over the 0–10 d post-UAN period. Points represent individual UAN events, and boxplots show the median and interquartile range. $S_{HAS}$ represents prognostic canopy HAS storage, $f_{wet,HAS}$ the RH-dependent effective HAS wet fraction, and $\beta_{HAS}$ the additional HAS evaporative efficiency term. Direct HAS water loss represents the simulated HAS flux, and the net effect on total transpiration represents the difference between ORC-HAS

https://doi.org/10.5194/egusphere-2026-6152
Preprint. Discussion started: 12 November 2026
© Author(s) 2026. CC BY 4.0 License.

and ORC-STD. The soil water feedback represents the net transpiration difference minus the direct HAS water loss.

### 3.2 Magnitude of simulated HAS effects and LE performance

ORC-HAS increased mean daily LE during the 0–10 d post-UAN period by 1.41–2.15 W $m^{-2}$ (2.0–4.0%) relative to ORC-STD across the four sites, while the mean fraction of direct HAS water loss offset by soil water feedback ranged from 13.3% to 24.9% (Table S7). Median $\Delta RMSE_{LE}$ ranged from −0.64 to −0.11 W $m^{-2}$ across the four sites, with lower RMSE under ORC-HAS in 61–100% of UAN events. At FR-Gri, LE was consistently underestimated, with smaller negative biases under ORC-HAS, whereas biases at BE-Lon remained closer to zero (Fig. 3a, d). $\Delta RMSE_{LE}$ was generally negative at FR-Gri but centered near zero at BE-Lon (Fig. 3b, e). Relative to ORC-STD, ORC-HAS improved RMSE, MAE, and absolute bias for LE across most UAN events at both sites, with less frequent improvements in $R^2$ (Fig. 3c, f). Window-length sensitivity analysis showed consistent $\Delta RMSE_{LE}$ across the 0–7 d, 0–10 d, and 0–14 d post-UAN windows (Fig. S3).

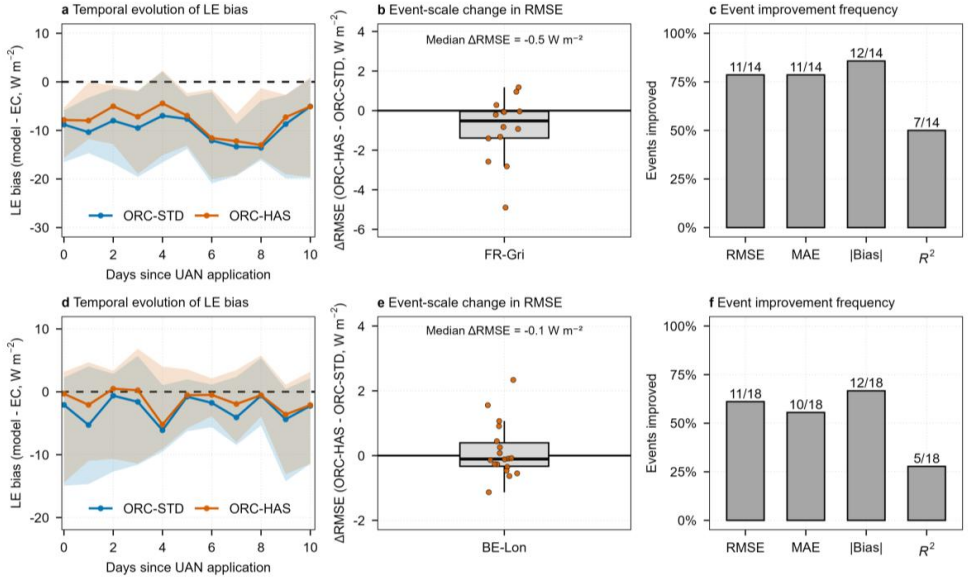



**Figure 3.** LE bias and event-scale performance after UAN application at FR-Gri (a–c) and BE-Lon (d–f). (a, d) Event-composite LE bias over 0–10 d after UAN application for ORC-STD and ORC-HAS, calculated relative to EC observations. Lines indicate event medians, and shaded ribbons indicate interquartile ranges across UAN events. (b, e) Event-scale change in $RMSE_{LE}$, calculated as ORC-HAS minus ORC-STD. Negative $\Delta RMSE_{LE}$ values indicate improved LE performance under ORC-HAS. Boxplots show the distribution across UAN events, with points representing individual events. (c, f) Percentage of UAN events in which ORC-HAS improved RMSE, MAE, absolute bias, and $R^2$ relative to ORC-STD.

https://doi.org/10.5194/egusphere-2026-6152
Preprint. Discussion started: 12 November 2026
© Author(s) 2026. CC BY 4.0 License.

### 3.3 Parameter sensitivity and process controls on simulated HAS responses

Sensitivity analyses showed consistent responses to $c_{RH}$, $\tau$, and $k_{wash}$ at FR-Gri and BE-Lon (Fig. 4). Increasing $c_{RH}$ and $\tau$ increased $f_{wet,HAS}$, $\beta_{HAS}$, and $\Delta LE_{HAS}$, whereas increasing $k_{wash}$ reduced these responses. $c_{RH}$ produced the largest relative variation, with ΔLEHAS changing by −42.6% to +35.3% at FR-Gri and −43.7% to +36.0% at BE-Lon relative to the reference simulation. The corresponding changes in LE performance were modest and did not alter the overall site-level patterns in $\Delta RMSE_{LE}$ (Fig. S4).

Diagnostic analyses further characterized the environmental and process controls on simulated HAS responses (Fig. S5). On non-overflow days, both RH and $S_{HAS}$ were positively associated with $f_{wet,HAS}$, with a stronger standardized effect of $S_{HAS}$ than RH at both sites. RH and $S_{HAS}$ jointly explained variation in $f_{wet,HAS}$ ($R^2$ = 0.76 and 0.64 at FR-Gri and BE-Lon, respectively). $S_{HAS}$ loss after accounting for dry depletion differed significantly among overflow classes at both sites (Kruskal–Wallis $p < 0.001$) and increased from non-overflow to high-overflow conditions, consistent with additional wash-off of canopy HAS storage. Event-mean $f_{wet,HAS}$ showed negative, non-significant correlations with $\Delta RMSE_{LE}$ at both sites. Under the prescribed water-deficit simulation (*humrel* = 0.5), the HAS-induced LE response remained positive but was reduced by 5.4% at FR-Gri and 12.0% at BE-Lon relative to the reference simulations (Fig. S6).

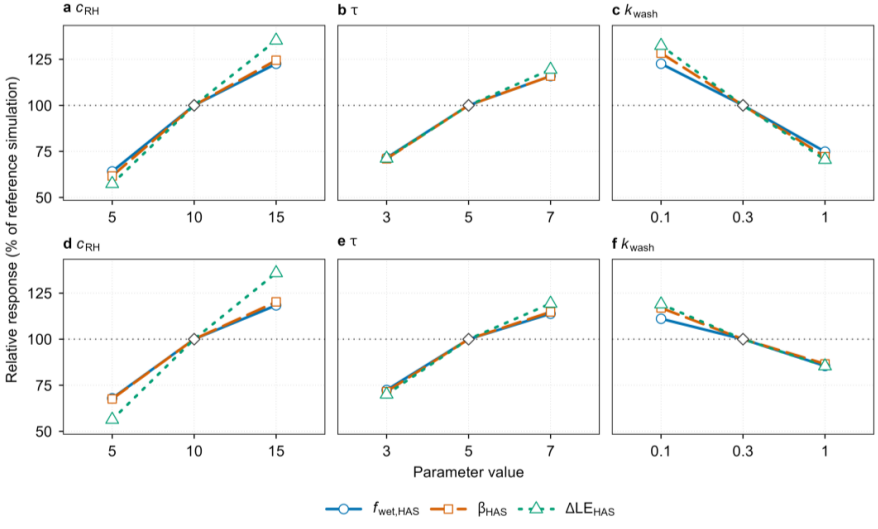



**Figure 4.** Sensitivity of simulated HAS responses to HAS parameters at FR-Gri (a–c) and BE-Lon (d–f). Panels show responses to the RH-scaling coefficient $c_{RH}$ (a, d), the dry depletion timescale $\tau$ (b, e), and the wash-off coefficient $k_{wash}$ (c, f). The relative responses of $f_{wet,HAS}$, $\beta_{HAS}$, and $\Delta LE_{HAS}$ are expressed as percentages of the reference simulation ($c_{RH}$ = 10, $\tau$ = 5 d, and $k_{wash}$ = 0.3 $m^2$ $kg^{-1}$). The horizontal dotted line indicates the reference level (100%). $\Delta LE_{HAS}$ denotes the mean difference between LE_ORC-HAS and LE_ORC-STD over the 0–10 d post-UAN event windows.

https://doi.org/10.5194/egusphere-2026-6152
Preprint. Discussion started: 12 November 2026
© Author(s) 2026. CC BY 4.0 License.

### 3.4 Diagnostic evaluation of IWUE responses

Simulated GPP was generally underestimated relative to EC observations during the post-UAN period at both FR-Gri and BE-Lon (Fig. 5a, d) and remained nearly identical between ORC-HAS and ORC-STD ($R^2 \approx 1.0$). Temporally, GPP differences remained near zero over the 10 d before and after UAN application, whereas the LE response emerged after application and generally declined (Fig. 5b, e).

Simulated IWUE was generally consistent with observed IWUE under both ORC-STD and ORC-HAS, although residual discrepancies remained (Fig. 5c, f). ORC-HAS showed modestly better agreement with observed IWUE than ORC-STD. Across the four study sites, simulated IWUE decreased by 4.0–5.3% relative to ORC-STD (Table S7).

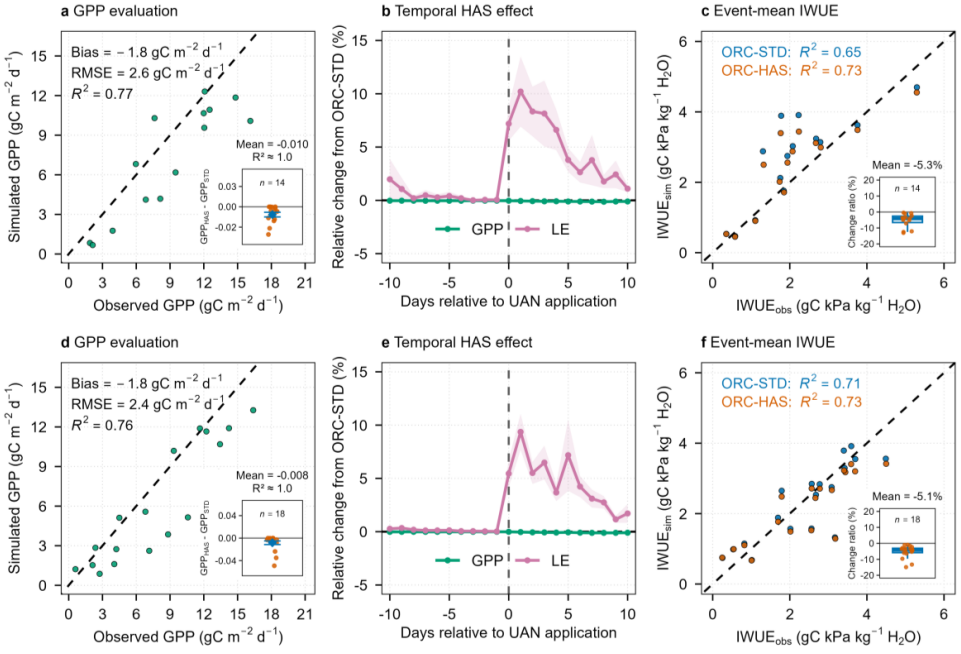



**Figure 5.** Diagnostic evaluation of GPP, LE, and IWUE during UAN event windows at FR-Gri (a–c) and BE-Lon (d–f). (a, d) Event-mean comparison of observed and simulated GPP during the 0–10 d post-UAN period. The dashed line indicates the 1:1 relationship. The inset shows the event-scale differences in simulated GPP between ORC-HAS and ORC-STD; $R^2$ indicates the agreement between the two simulations. (b, e) Temporal effect of ORC-HAS on simulated GPP and LE over the 10 d before and after UAN application, calculated as (ORC-HAS − ORC-STD) / ORC-STD × 100 for each event day. The vertical dashed line indicates the day of UAN application. Lines show event-composite means, and shaded ribbons indicate ±1 standard error across UAN events. (c, f) Event-mean comparison of observed and simulated IWUE during the 0–10 d post-UAN period for ORC-STD and ORC-HAS. The dashed line indicates the 1:1 relationship, and the inset shows the event-scale relative change in IWUE between ORC-HAS and ORC-STD.

https://doi.org/10.5194/egusphere-2026-6152
Preprint. Discussion started: 12 November 2026
© Author(s) 2026. CC BY 4.0 License.

# 4 Discussion

## 4.1 Process-based representation of UAN-induced HAS in ORCHIDEE-CROP

The HAS parameterization represents UAN-induced water loss as an event-driven, meteorologically regulated process and couples the resulting HAS flux to the soil water balance, allowing feedback on conventional transpiration. The calibrated reference UAN amount ($N_{ref}$) is an effective parameter controlling the conversion of retained UAN to HAS storage ($S_{HAS}$), whereas $c_{RH}$, $\tau$, and $k_{wash}$ represent unresolved canopy-scale variability in surface wetting, UAN residue persistence, and rainfall wash-off. These empirical parameters are required because the underlying canopy-scale processes cannot be directly constrained from available observations. The effective HAS wet fraction ($f_{wet,HAS}$) is particularly uncertain because leaf surface wetting and liquid water pathways through stomatal pores are spatially heterogeneous (Eichert et al., 2008; Katata and Held, 2021; Burkhardt et al., 2023), while hygroscopic residues vary in their spatial distribution, deliquescence relative humidity, and hygroscopic water uptake (Grantz, 1990; Burkhardt et al., 2012; Burkhardt and Pariyar, 2014). These uncertainties reflect the broader difficulty of isolating HAS-related water loss from EC observations (Deng et al., 2026).

The reference value $\tau$ = 5 d represents canopy HAS storage persistence under rain-free conditions. Its lower sensitivity bound ($\tau$ = 3 d) is close to the 2.88 d e-folding timescale used in previous ammonia exchange parameterizations (Massad et al., 2010; Flechard et al., 2013), while the 5–7 d settings allow for potentially longer persistence of UAN-derived hygroscopic residues. UAN residue persistence is likely to vary with environmental conditions, canopy properties, and residue composition. The sensitivity to $\tau$, $c_{RH}$, and $k_{wash}$ therefore highlights the need for better observational constraints on these empirical parameters (Fig. 4).

## 4.2 Event-dependent effects of HAS on simulated LE

ORC-HAS increased mean daily LE by 1.41–2.15 W m$^{-2}$ relative to ORC-STD during the 0–10 d post-UAN period across the four sites (Table S7). ORC-STD generally underestimated post-UAN LE, and the additional HAS flux reduced the negative bias, although underestimation remained. Whether this increase in LE improves agreement with EC observations depends on the ORC-STD bias and is also subject to EC measurement uncertainty. Temporal variations in LE additionally reflect meteorological forcing, vegetation phenology, canopy conductance, and surface energy partitioning (Wilson et al., 2002; Schulz and Jarvis, 2004; Bonan et al., 2014). At FR-Gri and BE-Lon, the additional HAS water loss reduced the soil moisture stress factor *humrel* (Fig. S2), thereby constraining conventional transpiration and partially offsetting the direct HAS contribution (Fig. 2d–e).

## 4.3 Process controls on simulated HAS responses

The stronger association of $f_{wet,HAS}$ with $S_{HAS}$ than with RH is consistent with the proposed role of hygroscopic leaf surface material in maintaining surface wetness (Fig. S5a, d; Burkhardt, 2010; Burkhardt and Pariyar, 2014; Burkhardt et al., 2023). Increased $S_{HAS}$ loss with canopy overflow is consistent with additional removal by rainfall wash-off beyond dry depletion (Fig. S5b, e). This process limits UAN residue persistence after

https://doi.org/10.5194/egusphere-2026-6152
Preprint. Discussion started: 12 November 2026
© Author(s) 2026. CC BY 4.0 License.

rainfall events and may contribute to variation in HAS responses, as comparable UAN inputs can produce different LE responses depending on post-application RH and canopy overflow.

The negative relationship between event-mean $f_{wet,HAS}$ and $\Delta RMSE_{LE}$ is consistent with the proposed HAS mechanism, whereby hygroscopic surface wetting may enhance the continuity of liquid water pathways through stomatal pores and facilitate HAS-related water loss (Fig. S5c, f; Burkhardt, 2010; Burkhardt et al., 2012; Grantz et al., 2018; Koch et al., 2025).

The reduced HAS-induced LE response under the prescribed water-deficit simulation indicates that soil water limitation can constrain the simulated HAS effect (Fig. S6). Lower *humrel* constrained conventional transpiration and also limited additional water loss through the HAS pathway, consistent with reduced canopy water exchange under water-limited conditions (Fang et al., 2021; Green et al., 2024).

### 4.4 IWUE interpretation and parameterization limitations

The decrease in simulated IWUE primarily reflected increased water loss rather than changes in carbon assimilation (Fig. 5; Table S7). This is consistent with the proposed HAS mechanism, whereby HAS introduces an additional liquid water-loss pathway that is distinct from conventional stomatal vapor diffusion and therefore not directly coupled to $CO_2$ uptake. HAS-induced water loss can nevertheless affect GPP indirectly through changes in soil water availability and associated water stress. *humrel* was generally above 0.9 during the 0–10 d post-UAN period, which also limited indirect effects of HAS water loss on GPP.

In addition to these water-mediated effects, UAN application may affect crop carbon assimilation through changes in nitrogen status and photosynthetic capacity. These effects are not represented in the current parameterization, in which event-based UAN inputs drive canopy HAS storage without altering the background fertilizer setting. Leaf surface traits may also influence film formation and HAS activation but are not explicitly represented in the current scheme (Fernández et al., 2017; Frank et al., 2025). The current framework may also be relevant to HAS associated with ambient hygroscopic aerosol deposition, but extending it beyond UAN would require parameterization based on aerosol properties. The scheme should therefore be interpreted as a process-based representation of an additional water-loss pathway rather than as a fully constrained description of leaf-scale HAS processes.

## 5 Conclusion

This study developed the first process-based representation of UAN-induced HAS in ORCHIDEE-CROP. The parameterization represents event-driven canopy retention, RH-dependent wetting, dry depletion, and rainfall wash-off of hygroscopic UAN residues and quantifies the resulting HAS-related water loss. The scheme produced transient post-UAN HAS responses and increased post-UAN LE across four temperate cropland sites. Process diagnostics and sensitivity analyses at FR-Gri and BE-Lon showed that the simulated response was controlled by retained UAN residues, RH, rainfall wash-off, and soil water limitation. Coupling HAS water loss to the soil water balance further showed that the direct HAS contribution was partially offset

https://doi.org/10.5194/egusphere-2026-6152
Preprint. Discussion started: 12 November 2026
© Author(s) 2026. CC BY 4.0 License.

by reduced conventional transpiration at both sites. Simulated GPP remained nearly unchanged, whereas increased water loss reduced simulated IWUE by approximately 5%. Overall, the study provides a framework for representing UAN-induced surface wetness and the associated water loss through HAS in land surface and crop models. More broadly, incorporating this process may help assess how hygroscopic fertilizer applications influence crop water use and soil water availability across agroecosystems. Future work should evaluate the scheme across other vegetation types, extend it to conditions of widespread hygroscopic aerosol deposition, and improve the representation of HAS in plant–atmosphere interactions.

## Code and data availability

The ORCHIDEE-CROP model code (v2.2), including the HAS parameterization, is archived on Zenodo at https://doi.org/10.5281/zenodo.23941910 (Deng, 2026c). The meteorological forcing data, crop management data, model experiment configurations, and scripts for data preprocessing, model output processing, parameter calibration, statistical analysis, and figure generation are archived on Zenodo at https://doi.org/10.5281/zenodo.23942703 (Deng, 2026a). The original ecosystem flux and meteorological data for FR-Gri, BE-Lon, and FR-EM2 are available from the Integrated Carbon Observation System (ICOS) Data Portal at https://hdl.handle.net/11676/XSI0ETkKyVVydpJuL7ro3_rQ (Buysse et al., 2026), https://hdl.handle.net/11676/1u2xQ5XcQoX0j2wJiZcyDP3M (Dumont et al., 2026), and https://hdl.handle.net/11676/tqY53lt1dCh3HZXtN-rLGEp5 (Leonard et al., 2026), respectively. The original ecosystem flux and meteorological data for US-Ne1 are available from the AmeriFlux FLUXNET data product at https://doi.org/10.17190/AMF/1871140 (Suyker, 2026). The eddy covariance and meteorological datasets used in this study have also been archived on Zenodo at https://doi.org/10.5281/zenodo.24085324 (Deng, 2026b) to support long-term accessibility and reproducibility.

## Author contributions

SD, JB, NV, BL, and JK conceptualized and designed the study. SD modified and implemented the HAS parameterization in ORCHIDEE-CROP, with YS, EB-F, and KY contributing methodological guidance on model development and implementation. SD performed the model simulations and formal analyses and led the writing of the original draft with contributions from all co-authors. BD provided site observations, meteorological data, and crop management information. BL, NV, RL, JB, and CF supervised the study. All authors participated in reviewing, editing, and finalizing the manuscript.

## Competing interests

The contact author has declared that none of the authors has any competing interests.

## Acknowledgements

The authors thank Carmen Kalalian, Joël Léonard, and Frederic Bornet for providing access to the ICOS ecosystem flux and site management data. We also thank Andy Suyker for providing the corresponding US-

https://doi.org/10.5194/egusphere-2026-6152
Preprint. Discussion started: 12 November 2026
© Author(s) 2026. CC BY 4.0 License.

Ne1 data through the AmeriFlux data platform. Shuaishuai Deng was funded by the China Scholarship Council (CSC). Jürgen Burkhardt was funded by the Deutsche Forschungsgemeinschaft (DFG, German Research Foundation; project number 446535617). Ronny Lauerwald was supported by the CLand Convergence Institute (16-CONV-0003), funded by the French National Research Agency (ANR). Jürgen Knauer acknowledges support from the UTS Chancellor's Research Fellowship.

**References**

Ball, J. T., Woodrow, I. E., and Berry, J. A.: A model predicting stomatal conductance and its contribution to the control of photosynthesis under different environmental conditions, in: Progress in Photosynthesis Research, edited by: Biggins, J., Springer Netherlands, Dordrecht, 221–224, https://doi.org/10.1007/978-94-017-0519-6_48, 1987.

Barlas, N. T., Bahamonde, H. A., Pimentel, C., Domínguez-Huidobro, P., Pina, C. M., and Fernández, V.: Evaluating leaf wettability and salt hygroscopicity as drivers for foliar absorption, Plants, 12, 2357, https://doi.org/10.3390/plants12122357, 2023.

Beer, C., Ciais, P., Reichstein, M., Baldocchi, D., Law, B. E., Papale, D., Soussana, J. -F., Ammann, C., Buchmann, N., Frank, D., Gianelle, D., Janssens, I. A., Knohl, A., Köstner, B., Moors, E., Roupsard, O., Verbeeck, H., Vesala, T., Williams, C. A., and Wohlfahrt, G.: Temporal and among-site variability of inherent water use efficiency at the ecosystem level, Glob. Biogeochem. Cycles, 23, 2008GB003233, https://doi.org/10.1029/2008GB003233, 2009.

Bonan, G.: Climate change and terrestrial ecosystem modeling, 1st ed., Cambridge University Press, https://doi.org/10.1017/9781107339217, 2019.

Bonan, G. B., Williams, M., Fisher, R. A., and Oleson, K. W.: Modeling stomatal conductance in the earth system: linking leaf water-use efficiency and water transport along the soil–plant–atmosphere continuum, Geosci. Model Dev., 7, 2193–2222, https://doi.org/10.5194/gmd-7-2193-2014, 2014.

Brisson, N., Gary, C., Justes, E., Roche, R., Mary, B., Ripoche, D., Zimmer, D., Sierra, J., Bertuzzi, P., Burger, P., Bussière, F., Cabidoche, Y. M., Cellier, P., Debaeke, P., Gaudillère, J. P., Hénault, C., Maraux, F., Seguin, B., and Sinoquet, H.: An overview of the crop model STICS, Eur. J. Agron., 18, 309–332, https://doi.org/10.1016/S1161-0301(02)00110-7, 2003.

Brisson, N., Launay, M., Mary, B., and Beaudoin, N.: Conceptual basis, formalisations and parameterization of the STICS crop model, Ed. Quae, Versailles, https://www.quae.com/product/1022/9782759209712/conceptual-basis-formalisations-and-parameterization-of-the-stics-crop-model, 2009.

Brunauer, S., Emmett, P. H., and Teller, E.: Adsorption of gases in multimolecular layers, J. Am. Chem. Soc., 60, 309–319, https://doi.org/10.1021/ja01269a023, 1938.

Burkhardt, J.: Hygroscopic particles on leaves: nutrients or desiccants?, Ecol. Monogr., 80, 369–399, https://doi.org/10.1890/09-1988.1, 2010.

Burkhardt, J. and Pariyar, S.: Particulate pollutants are capable to 'degrade' epicuticular waxes and to

https://doi.org/10.5194/egusphere-2026-6152
Preprint. Discussion started: 12 November 2026
© Author(s) 2026. CC BY 4.0 License.

decrease the drought tolerance of Scots pine (*Pinus sylvestris* L.), Environ. Pollut., 184, 659–667, https://doi.org/10.1016/j.envpol.2013.04.041, 2014.

Burkhardt, J. and Pariyar, S.: How does the VPD response of isohydric and anisohydric plants depend on leaf surface particles?, Plant Biol., 18, 91–100, https://doi.org/10.1111/plb.12402, 2016.

Burkhardt, J., Peters, K., and Crossley, A.: The presence of structural surface waxes on coniferous needles affects the pattern of dry deposition of fine particles, J. Exp. Bot., 46, 823–831, https://doi.org/10.1093/jxb/46.7.823, 1995.

Burkhardt, J., Flechard, C. R., Gresens, F., Mattsson, M., Jongejan, P. A. C., Erisman, J. W., Weidinger, T., Meszaros, R., Nemitz, E., and Sutton, M. A.: Modelling the dynamic chemical interactions of atmospheric ammonia with leaf surface wetness in a managed grassland canopy, Biogeosciences, 6, 67–84, https://doi.org/10.5194/bg-6-67-2009, 2009.

Burkhardt, J., Basi, S., Pariyar, S., and Hunsche, M.: Stomatal penetration by aqueous solutions – an update involving leaf surface particles, New Phytol., 196, 774–787, https://doi.org/10.1111/j.1469-8137.2012.04307.x, 2012.

Burkhardt, J., Zinsmeister, D., Grantz, D. A., Vidic, S., Sutton, M. A., Hunsche, M., and Pariyar, S.: Camouflaged as degraded wax: hygroscopic aerosols contribute to leaf desiccation, tree mortality, and forest decline, Environ. Res. Lett., 13, 085001, https://doi.org/10.1088/1748-9326/aad346, 2018.

Burkhardt, J., Zinsmeister, D., Roth-Nebelsick, A., Hüging, H., and Pariyar, S.: Ambient aerosols increase stomatal transpiration and conductance of hydroponic sunflowers by extending the hydraulic system to the leaf surface, Front. Plant Sci., 14, 1275358, https://doi.org/10.3389/fpls.2023.1275358, 2023.

Buysse, P., Loubet, B., Depuydt, J., Durand, B., Gueudet, J.-C., and Kalalian, C.: Fluxnet archive product from Grignon, 2004-01-01–2026-09-06, Ecosystem Thematic Centre [data set], https://hdl.handle.net/11676/XSI0ETkKyVVydpJuL7ro3_rQ, 2026.

Cao, P., Lu, C., and Yu, Z.: Historical nitrogen fertilizer use in agricultural ecosystems of the contiguous United States during 1850–2015: application rate, timing, and fertilizer types, Earth Syst. Sci. Data, 10, 969–984, https://doi.org/10.5194/essd-10-969-2018, 2018.

Deng, S.: A process-based representation of hydraulic activation of stomata induced by hygroscopic fertilizer salts in the ORCHIDEE-CROP model (v2.2), Zenodo [data set], https://doi.org/10.5281/zenodo.23942703, 2026a.

Deng, S.: FLUXNET observational data for agricultural sites, Zenodo [data set], https://doi.org/10.5281/zenodo.24085324, 2026b.

Deng, S.: ORCHIDEE-CROP v2.2: ORCHIDEE-CROP-HAS, Zenodo [code], https://doi.org/10.5281/zenodo.23941910, 2026c.

Deng, S., Burkhardt, J., Lauerwald, R., Flechard, C., Knauer, J., Kalalian, C., Dumont, B., Mauder, M., Brümmer, C., Viovy, N., and Loubet, B.: Hydraulic activation of stomata induced by hygroscopic fertilizer salts alters crop carbon–water exchange: field evidence from cereal crops, Plant Cell Environ., 49, 10012–10023, https://doi.org/10.1111/pce.70870, 2026.

https://doi.org/10.5194/egusphere-2026-6152
Preprint. Discussion started: 12 November 2026
© Author(s) 2026. CC BY 4.0 License.



587 Dumont, B., Heinesch, B., Bodson, B., Bogaerts, G., Chopin, H., De Ligne, A., Demoulin, L., Douxfils, B.,
588 Engelmann, T., Faurès, A., Longdoz, B., Manise, T., Orgun, A., Piret, A., and Thyrion, T.: Fluxnet
589 archive product from Lonzee, 2004–2024, Ecosystem Thematic Centre [data set],
590 https://hdl.handle.net/11676/1u2xQ5XcQoX0j2wJiZcyDP3M, 2026.
591 EFSA: EFSA guidance document for predicting environmental concentrations of active substances of plant
592 protection products and transformation products of these active substances in soil, EFSA J., 15,
593 https://doi.org/10.2903/j.efsa.2017.4982, 2017.
594 Eichert, T., Kurtz, A., Steiner, U., and Goldbach, H. E.: Size exclusion limits and lateral heterogeneity of the
595 stomatal foliar uptake pathway for aqueous solutes and water-suspended nanoparticles, Physiol. Plant.,
596 134, 151–160, https://doi.org/10.1111/j.1399-3054.2008.01135.x, 2008.
597 Fang, Y., Leung, L. R., Wolfe, B. T., Detto, M., Knox, R. G., McDowell, N. G., Grossiord, C., Xu, C.,
598 Christoffersen, B. O., Gentine, P., Koven, C. D., and Chambers, J. Q.: Disentangling the effects of vapor
599 pressure deficit and soil water availability on canopy conductance in a seasonal tropical forest during
600 the 2015 el niño drought, J. Geophys. Res. Atmos., 126, e2021JD035004,
601 https://doi.org/10.1029/2021JD035004, 2021.
602 Farquhar, G. D., Von Caemmerer, S., and Berry, J. A.: A biochemical model of photosynthetic $CO_2$
603 assimilation in leaves of C3 species, Planta, 149, 78–90, https://doi.org/10.1007/BF00386231, 1980.
604 Fernández, V., Bahamonde, H. A., Peguero-Pina, J. J., Gil-Pelegrín, E., Sancho-Knapik, D., Gil, L., Goldbach,
605 H. E., and Eichert, T.: Physico-chemical properties of plant cuticles and their functional and ecological
606 significance, J. Exp. Bot., 68, 5293–5306, https://doi.org/10.1093/jxb/erx302, 2017.
607 Flechard, C. R., Massad, R.-S., Loubet, B., Personne, E., Simpson, D., Bash, J. O., Cooter, E. J., Nemitz, E.,
608 and Sutton, M. A.: Advances in understanding, models and parameterizations of biosphere-atmosphere
609 ammonia exchange, Biogeosciences, 10, 5183–5225, https://doi.org/10.5194/bg-10-5183-2013, 2013.
610 Frank, M., Kristensen, E. V., Szameitat, A., Siracusa, F., Ertem, I., Dahl, R., Dempsey, K. G., Mokso, R.,
611 and Husted, S.: X-ray micro- CT imaging to study foliar water uptake mechanisms in plants with
612 contrasting leaf topography, New Phytol., 248, 656–671, https://doi.org/10.1111/nph.70421, 2025.
613 Fu, J., Jian, Y., Wang, X., Li, L., Ciais, P., Zscheischler, J., Wang, Y., Tang, Y., Müller, C., Webber, H.,
614 Yang, B., Wu, Y., Wang, Q., Cui, X., Huang, W., Liu, Y., Zhao, P., Piao, S., and Zhou, F.: Extreme
615 rainfall reduces one-twelfth of China's rice yield over the last two decades, Nat. Food, 4, 416–426,
616 https://doi.org/10.1038/s43016-023-00753-6, 2023.
617 Grantz, D. A.: Plant response to atmospheric humidity, Plant Cell Environ., 13, 667–679,
618 https://doi.org/10.1111/j.1365-3040.1990.tb01082.x, 1990.
619 Grantz, D. A., Zinsmeister, D., and Burkhardt, J.: Ambient aerosol increases minimum leaf conductance and
620 alters the aperture–flux relationship as stomata respond to vapor pressure deficit (VPD), New Phytol.,
621 219, 275–286, https://doi.org/10.1111/nph.15102, 2018.
622 Green, J. K., Zhang, Y., Luo, X., and Keenan, T. F.: Systematic underestimation of canopy conductance
623 sensitivity to drought by earth system models, AGU Adv., 5, e2023AV001026,

https://doi.org/10.5194/egusphere-2026-6152
Preprint. Discussion started: 12 November 2026
© Author(s) 2026. CC BY 4.0 License.

https://doi.org/10.1029/2023AV001026, 2024.

Katata, G. and Held, A.: Combined measurements of microscopic leaf wetness and dry-deposited inorganic compounds in a spruce forest, Atmos. Pollut. Res., 12, 217–224, https://doi.org/10.1016/j.apr.2020.11.004, 2021.

Koch, I., Kahmen, A., and Burkhardt, J.: Aerosol deposition affects water uptake and water loss of beech leaves, Tree Physiol., 45, tpaf055, https://doi.org/10.1093/treephys/tpaf055, 2025.

Krinner, G., Viovy, N., De Noblet-Ducoudré, N., Ogée, J., Polcher, J., Friedlingstein, P., Ciais, P., Sitch, S., and Prentice, I. C.: A dynamic global vegetation model for studies of the coupled atmosphere-biosphere system, Glob. Biogeochem. Cycles, 19, 2003GB002199, https://doi.org/10.1029/2003GB002199, 2005.

Leonard, J., Bornet, F., François, B., and Grehan, E.: Fluxnet archive product from Estrees-Mons A28, 2017–2025, Ecosystem Thematic Centre [data set], https://hdl.handle.net/11676/tqY53lt1dCh3HZXtN-rLGEp5, 2026.

Lu, C. and Tian, H.: Global nitrogen and phosphorus fertilizer use for agriculture production in the past half century: shifted hot spots and nutrient imbalance, Earth Syst. Sci. Data, 9, 181–192, https://doi.org/10.5194/essd-9-181-2017, 2017.

Massad, R.-S., Nemitz, E., and Sutton, M. A.: Review and parameterisation of bi-directional ammonia exchange between vegetation and the atmosphere, Atmos. Chem. Phys., 10, 10359–10386, https://doi.org/10.5194/acp-10-10359-2010, 2010.

Medlyn, B. E., Duursma, R. A., Eamus, D., Ellsworth, D. S., Prentice, I. C., Barton, C. V. M., Crous, K. Y., De Angelis, P., Freeman, M., and Wingate, L.: Reconciling the optimal and empirical approaches to modelling stomatal conductance, Glob. Change Biol., 17, 2134–2144, https://doi.org/10.1111/j.1365-2486.2010.02375.x, 2011.

Müller, C., Elliott, J., Chryssanthacopoulos, J., Arneth, A., Balkovic, J., Ciais, P., Deryng, D., Folberth, C., Glotter, M., Hoek, S., Iizumi, T., Izaurralde, R. C., Jones, C., Khabarov, N., Lawrence, P., Liu, W., Olin, S., Pugh, T. A. M., Ray, D. K., Reddy, A., Rosenzweig, C., Ruane, A. C., Sakurai, G., Schmid, E., Skalsky, R., Song, C. X., Wang, X., De Wit, A., and Yang, H.: Global gridded crop model evaluation: benchmarking, skills, deficiencies and implications, Geosci. Model Dev., 10, 1403–1422, https://doi.org/10.5194/gmd-10-1403-2017, 2017.

Müller, C., Elliott, J., Kelly, D., Arneth, A., Balkovic, J., Ciais, P., Deryng, D., Folberth, C., Hoek, S., Izaurralde, R. C., Jones, C. D., Khabarov, N., Lawrence, P., Liu, W., Olin, S., Pugh, T. A. M., Reddy, A., Rosenzweig, C., Ruane, A. C., Sakurai, G., Schmid, E., Skalsky, R., Wang, X., De Wit, A., and Yang, H.: The global gridded crop model intercomparison phase 1 simulation dataset, Sci. Data, 6, 50, https://doi.org/10.1038/s41597-019-0023-8, 2019.

Schulz, K. and Jarvis, A. J.: Environmental and biological controls on the seasonal variations in latent heat fluxes derived from flux data for three forest sites, Water Resour. Res., 40, 2004WR003155, https://doi.org/10.1029/2004WR003155, 2004.

Su, Y., Lauerwald, R., Makowski, D., Viovy, N., Guilpart, N., Zhu, P., Gabrielle, B., and Ciais, P.: Future

https://doi.org/10.5194/egusphere-2026-6152
Preprint. Discussion started: 12 November 2026
© Author(s) 2026. CC BY 4.0 License.

warming increases the chance of success of maize-wheat double cropping in Europe, Eur. J. Agron., 170, 127723, https://doi.org/10.1016/j.eja.2025.127723, 2025.

Suyker, A.: AmeriFlux FLUXNET-1F US-Ne1 Mead - irrigated continuous maize site (v1.3_r1), AmeriFlux AMP [data set], https://doi.org/10.17190/AMF/1871140, 2026.

Tredenick, E. C., Stuart-Williams, H., and Enge, T. G.: Materials on plant leaf surfaces are deliquescent in a variety of environments, Front. Plant Sci., 13, 722710, https://doi.org/10.3389/fpls.2022.722710, 2022.

Wang, J., Zhou, Y., Liu, L., Zohner, C. M., Wei, J., and Wu, C.: Particulate air pollution undermines plant water-use efficiency by inhibiting photosynthesis, Nat. Clim. Change, 16, 1068–1074, https://doi.org/10.1038/s41558-026-02712-y, 2026.

Wang, X., Ciais, P., Li, L., Ruget, F., Vuichard, N., Viovy, N., Zhou, F., Chang, J., Wu, X., Zhao, H., and Piao, S.: Management outweighs climate change on affecting length of rice growing period for early rice and single rice in China during 1991–2012, Agric. For. Meteorol., 233, 1–11, https://doi.org/10.1016/j.agrformet.2016.10.016, 2017.

Wang, X., Müller, C., Elliot, J., Mueller, N. D., Ciais, P., Jägermeyr, J., Gerber, J., Dumas, P., Wang, C., Yang, H., Li, L., Deryng, D., Folberth, C., Liu, W., Makowski, D., Olin, S., Pugh, T. A. M., Reddy, A., Schmid, E., Jeong, S., Zhou, F., and Piao, S.: Global irrigation contribution to wheat and maize yield, Nat. Commun., 12, 1235, https://doi.org/10.1038/s41467-021-21498-5, 2021.

Weston, C. W., Papcun, J. R., and Dery, M.: Ammonium compounds, in: Kirk-Othmer Encyclopedia of Chemical Technology, edited by: Kirk-Othmer, Wiley, https://doi.org/10.1002/0471238961.0113131523051920.a01.pub2, 2003.

Wilson, K. B., Baldocchi, D. D., Aubinet, M., Berbigier, P., Bernhofer, C., Dolman, H., Falge, E., Field, C., Goldstein, A., Granier, A., Grelle, A., Halldor, T., Hollinger, D., Katul, G., Law, B. E., Lindroth, A., Meyers, T., Moncrieff, J., Monson, R., Oechel, W., Tenhunen, J., Valentini, R., Verma, S., Vesala, T., and Wofsy, S.: Energy partitioning between latent and sensible heat flux during the warm season at FLUXNET sites, Water Resour. Res., 38, 1249, https://doi.org/10.1029/2001WR000989, 2002.

Wu, X., Vuichard, N., Ciais, P., Viovy, N., De Noblet-Ducoudré, N., Wang, X., Magliulo, V., Wattenbach, M., Vitale, L., Di Tommasi, P., Moors, E. J., Jans, W., Elbers, J., Ceschia, E., Tallec, T., Bernhofer, C., Grünwald, T., Moureaux, C., Manise, T., Ligne, A., Cellier, P., Loubet, B., Larmanou, E., and Ripoche, D.: ORCHIDEE-CROP (v0), a new process-based agro-land surface model: model description and evaluation over Europe, Geosci. Model Dev., 9, 857–873, https://doi.org/10.5194/gmd-9-857-2016, 2016.

Yin, Z., Wang, X. H., Ottlé, C., Zhou, F., Guimberteau, M., Polcher, J., Peng, S. S., Piao, S. L., Li, L., Bo, Y., Chen, X. L., Zhou, X. D., Kim, H., and Ciais, P.: Improvement of the irrigation scheme in the ORCHIDEE land surface model and impacts of irrigation on regional water budgets over china, J. Adv. Model. Earth Syst., 12, e2019MS001770, https://doi.org/10.1029/2019MS001770, 2020.

Yu, K., Su, Y., Lauerwald, R., Ciais, P., Xi, Y., Xu, H., Zhang, X., Viovy, N., Pickering, A., Collard, M., and Goll, D. S.: Resolving effects of leaf pigmentation changes and plant residue on the energy balance

https://doi.org/10.5194/egusphere-2026-6152
Preprint. Discussion started: 12 November 2026
© Author(s) 2026. CC BY 4.0 License.



of winter wheat cultivation in the ORCHIDEE-CROP model, Geosci. Model Dev., 19, 7217–7237, https://doi.org/10.5194/gmd-19-7217-2026, 2026.